

Variability-sustained pattern formation in subexcitable media

Erik Glatt, Martin Gassel, and Friedemann Kaiser

Institute of Applied Physics, Darmstadt University of Technology, 64289 Darmstadt, Germany

(Received 9 November 2006; published 9 February 2007)

Starting with a subexcitable net of FitzHugh-Nagumo elements it is shown that parameter variability (diversity) is able to induce pattern formation. These patterns are most coherent for an intermediate variability strength. This effect is similar to the well-known spatiotemporal stochastic resonance generated by additive noise in subexcitable media. Furthermore, variability is able to induce a transition to an excitable behavior of the net. This transition strongly depends on the coupling strength between the elements and it is found only for strong coupling. For weaker coupling one observes a lifetime lengthening of waves propagating through the medium, but the net stays subexcitable.

DOI: [10.1103/PhysRevE.75.026206](https://doi.org/10.1103/PhysRevE.75.026206)

PACS number(s): 47.54.-r, 05.40.-a, 05.70.Fh

I. INTRODUCTION

Spatiotemporal pattern formation in excitable and subexcitable media has been investigated for many years. Already in 1995 Jung and Mayer-Kress studied the emergence of waves in an excitable cellular-automata-like system under the influence of additive white noise [1]. The existence of noise-sustained waves has been confirmed experimentally in slices of hippocampal astrocytes [2]. Further studies on pattern formation in subexcitable media under the influence of additive noise have been performed, e.g., in the Barkley system [3]. The additive noise introduces a nonzero probability for each element in the medium to become excited. These excitations spread out and pattern formation (wave propagation) can be observed. Similar to the effect of coherence resonance [4] one gets the most coherent system response (patterns) for an intermediate noise strength. This pattern formation is a stochastic resonance effect, known as spatiotemporal stochastic resonance (STSR). Noise-induced pattern formation is also studied, theoretically and experimentally, in the presence of multiplicative noise instead of additive noise [5,6]. Multiplicative noise can be handled analytically by applying Novikov's theorem [7]. The resulting deterministic equation describes the systematic influence of the noise on the system dynamics. This systematic effect can induce phase transitions in spatially extended systems [8–10].

In contrast to noise, internal variability (diversity) denotes static stochastic differences between the otherwise equal elements of a net. Such differences can influence the spatiotemporal dynamics. The influence of variability on the synchronization of coupled oscillators was investigated by Winfree [11] and Kuramoto [12]. These results are the basis for most of the studies on synchronization even today [13]. Variability influences spatiotemporal chaos [14] and can play an important role for pattern formation in a net of biochemical oscillators [15]. Furthermore, variability may have a systematic effect, which can induce transitions between different dynamical regimes [16]. Recently it was demonstrated that diversity can cause resonancelike phenomena in networks of nonlinear elements [17].

In the present paper the influence of variability on subexcitable nets of FitzHugh-Nagumo (FHN) elements is discussed [18]. It is shown that variability can induce pattern

formation in such nets. These patterns are most coherent for intermediate variability strength. It is demonstrated that variability can induce a transition from subexcitable to excitable net dynamics for large coupling strengths. For a weaker coupling no transition is observed, but the lifetime of waves in the medium can be enlarged by an appropriate amount of variability.

II. THE MODEL

The system under consideration is a net of $N \times N$ coupled FHN elements in the presence of variability in the parameters e and c ,

$$\begin{aligned} \dot{u}_{ij} &= \frac{1}{\epsilon} [u_{ij}(1 - u_{ij})(u_{ij} - a) - v_{ij} + d] + qK_{ij}, \\ \dot{v}_{ij} &= u_{ij} - c_{ij}v_{ij} + e_{ij}, \end{aligned} \quad (1)$$

where K_{ij} and q denote the coupling function and strength, respectively. In this minimal model of neural dynamics $u_{ij}(t)$ represents the fast relaxing membrane potential, while $v_{ij}(t)$ mimics the slow potassium gating variable. The more realistic Hodgkin-Huxley model [19] has a more complicated nonlinear voltage dependency in the corresponding variables. In the FHN model, which describes essential parts of the Hodgkin-Huxley model quite well, this nonlinearity in \dot{u}_{ij} is approximated by a cubic function and \dot{v}_{ij} is linearized in the relevant region of the parameter space. The parameters e and c in the FHN model are results of this linearization and have no direct counterpart in the Hodgkin-Huxley model. Other minimal models of neuronal dynamics are also of relevance, e.g., a direct reduction of the four-variable Hodgkin-Huxley model [19].

The integration time is specified in time units (t.u.) and the time scales are separated by the small parameter $\epsilon = 0.01$. The equations are integrated on a discrete spatiotemporal grid using the Heun method ($\Delta t = 0.001$ t.u.) [8] and the forward time centered space scheme ($\Delta h = 1.0$) in time and space, respectively. The integration in space is performed using periodic boundary conditions. The grid points are labeled by the indices $1 \leq i, j \leq N$. In order to study pattern formation and signal transmission through the net, the func-

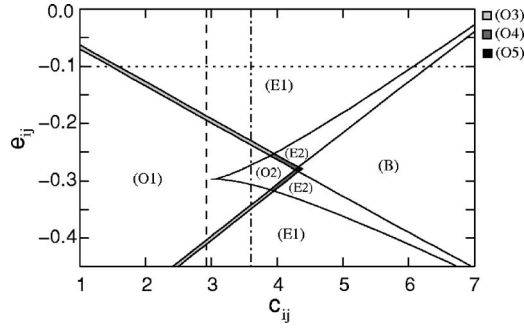


FIG. 1. Stability analysis of one FitzHugh-Nagumo element [Eq. (1)] dependent on its parameter values c_{ij} and e_{ij} . (a, d) = (0.01, -0.06). (—) boundaries of the dynamical regimes, (---) $c_{ij} = 2.93$, (- - -) $c_{ij} = 3.6$, ($\cdot \cdot \cdot$) $e_{ij} = -0.1$. E1 has one stable fixed point (excitable regime). E2 is like E1, and additionally has two unstable fixed points. O1 has one unstable fixed point and one stable limit cycle (oscillatory regime). O2 is like O1, with additionally two unstable fixed points. O3 has one stable fixed point and one stable limit cycle. O4 is like O3, with additionally two unstable fixed points. B shows two stable fixed points and one unstable fixed point (bistable regime). O5 is like B with additionally one stable limit cycle. Unstable limit cycles are not mentioned.

tion K_{ij} is chosen as diffusive nearest-neighbor coupling, using a nine-point Laplacian for radial symmetry,

$$K_{ij} = \nabla^2 u_{ij},$$

$$\nabla^2 u_{ij} = \frac{1}{6} [u_{i+1,j+1} + u_{i+1,j-1} + u_{i-1,j+1} + u_{i-1,j-1} + 4(u_{i+1,j} + u_{i-1,j} + u_{i,j+1} + u_{i,j-1}) - 20u_{ij}]. \quad (2)$$

The stability analysis of a single FHN element (ij th element) is presented in Fig. 1. The most important parameter regimes E1, O1, and B are well known and often discussed in the literature. Additionally one finds other dynamical regimes in small regions of the parameter space. Starting from the oscillatory regime O1 with one stable limit cycle and one unstable focus, increasing c_{ij} for $e_{ij} = -0.1$ leads to a stabilization of the focus. Now the regime O3 is realized. Both attractors are separated by an unstable limit cycle. A further increase of c_{ij} enlarges the area of attraction of the focus and at the border to the excitable regime E1 the limit cycles disappear. Once in the regime E1, increasing c_{ij} leads to a bifurcation, where a saddle point and an unstable focus arise in addition to the stable focus. This regime is called E2. A further increase of c_{ij} stabilizes the unstable focus and the bistable regime B emerges. It is also possible to find a dynamical regime with three unstable fixed points, two unstable foci and a saddle point, all of them inside a stable limit cycle. This regime is called O2. It should be possible to understand the other dynamical regimes with the information given.

In the present contribution only variability in the slow variables $v_{ij}(t)$ is considered. Due to the variability the values (c_{ij} and e_{ij}) of the parameters c and e can change from element to element. The parameter values are Gaussian-distributed numbers, with

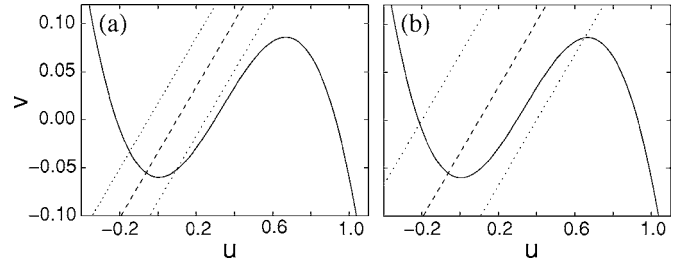


FIG. 2. Nullclines for one FitzHugh-Nagumo element [Eq. (1)]; (—) cubic nullcline, (- -) linear nullcline for $e_{ij} = E$. ($\cdot \cdot \cdot$) linear nullclines for $e_{ij} =$ (a) $E \pm 0.15$; (b) $E \pm 0.30$. Other parameters: $c_{ij} = 2.93$.

$$\langle e_{ij} \rangle = E, \quad \langle (e_{ij} - E)(e_{kl} - E) \rangle = \sigma_{va}^2 \delta_{ij,kl},$$

$$\langle c_{ij} \rangle = C, \quad \langle (c_{ij} - C)(c_{kl} - C) \rangle = \sigma_{vm}^2 \delta_{ij,kl}. \quad (3)$$

In the following σ_{vm}^2 , the variance of the Gaussian distribution $P(c, \sigma_{vm})$, and σ_{va}^2 , the variance of the Gaussian distribution $P(e, \sigma_{va})$, are denoted as variability intensities, whereas σ_{vm} and σ_{va} are denominated as variability strengths.

In the following the variability in the parameter e is called *additive variability*, because this parameter is an additive term in the differential equation [Eq. (1)]. This is different for the parameter c , which is multiplied by the system variables v_{ij} . Hence the variability in this parameter is called *multiplicative variability*.

Throughout this text the following set of parameters is used: (a, d, E, N) = (0.01, -0.06, -0.1, 256), while the variability strengths σ_{va} and σ_{vm} , the parameter C , and the coupling strength q are varied.

In the following a net is called excitable if a spatially uniform temporally constant solution is stable and a small excitation can induce an excitation wave, which is sustained in the net. If the wave dies out after some time, the net is called subexcitable. In this paper these expressions are also used for finite nets in the presence of variability, even if in these cases small fluctuations around the ideal homogeneous solution occur.

III. ADDITIVE VARIABILITY

In this section we use the fixed parameter values $q=20$, $C=2.93$, and $\sigma_{vm}=0$. Only the additive variability strength σ_{va} is varied. For the chosen parameters and without variability each FHN element is in the excitable regime (Fig. 1), resulting in a spatially uniform temporally constant solution for Eq. (1) and any initial conditions. Waves are not sustained in the absence of variability and thus the net is subexcitable.

Introducing additive variability in the net, the parameter values e_{ij} change from element to element. A change in this parameter shifts the linear nullcline of a FHN element (Fig. 2). Variability in the parameter d , which is also additive variability, would shift the cubic nullcline instead of the linear one. For the observed phenomena it is not important which nullcline is shifted and all the results presented in this section

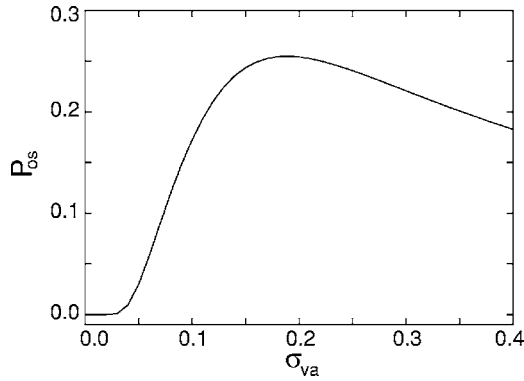


FIG. 3. Probability P_{os} for one FitzHugh-Nagumo element [Eq. (1)] to be in the oscillatory regime ($-0.194 > e_{ij} > -0.403$), dependent on the variability strength σ_{va} . Other parameters: $c_{ij}=2.93$.

can also be found for variability in the parameter d . The shift of the nullcline has a strong influence on its dynamics. This is demonstrated by the stability analysis in Fig. 1. For $e_{ij} > -0.187$ the element has only one stable fixed point (excitable regime). In this case a small excitation can stimulate a large loop in the phase space (single spike) before the element goes back to the fixed point. For the parameter range $-0.194 > e_{ij} > -0.403$, the element has one unstable fixed point surrounded by a stable limit cycle (oscillatory regime). Other dynamical regimes are also possible for appropriate values of e_{ij} . This discussion shows that the net [Eq. (1)] with variability in the parameter e may consist of elements in different dynamical regimes. The probability of an element to be in a certain regime depends on σ_{va} ; this is shown for the oscillatory regime in Fig. 3. In a net of Hodgkin-Huxley elements [20] the additive variability, studied in the present contribution, would mean that the nullclines $n_{ij}(V)$ of the gating variable n differ from element to element. Those nullclines are shifted to different values of the voltage V , while their shape is conserved. Variability in the parameter d , which means additive variability in the fast variable, would be variability in the parameter I of the Hodgkin-Huxley model, but one has to notice that changing I also changes the shape of the nullcline.

The influence of additive noise on pattern formation has been studied in detail (e.g., [1–3]). For weak noise strengths

the probability of an element to get excited by the noise is almost zero and no pattern formation can be observed. This behavior changes abruptly if a certain threshold of the noise strength is reached. Now there is a much higher probability for each element in the medium to become excited. These excitations spread out in the net and pattern formation (wave propagation) can be observed. The most coherent patterns are observed for an intermediate noise strength (STSR), because for higher noise strengths the coherent patterns are destroyed.

Since in the present contribution the additive noise is replaced by variability in parameter e one has instead of a stochastic external forcing a diverse net. The influence of the variability on the observed pattern formation is shown in Fig. 4. For a small variability strength ($\sigma_{va} < 0.12$) no pattern formation can be observed [Fig. 4(b)], whereas for a slightly larger variability strength one observes the development of wave fronts, which spread through the net [Fig. 4(c)]. A further increase of the variability strength leads to a destruction of the large coherent structures [Fig. 4(d)].

To quantify the coherence of the variability-induced patterns the spatial cross correlation S of the variables u_{ij} is used [3]. It is defined as the space- and time-averaged nearest-neighbor amplitude distance of all elements $K(t)$ (spatial autocovariance) normalized by the total spatial amplitude variance $V(t)$, which is defined as

$$V(t) = \frac{1}{N^2} \sum_{ij} (u_{ij} - \bar{u})^2, \quad (4)$$

where \bar{u} denotes the mean value of the fast variable at time t for all elements (mean field). The spatial autocovariance of the nearest neighbors can be written as

$$K(t) = \frac{1}{N^2} \sum_{ij} \frac{1}{N_{ij}} \sum_{b \in N_{ij}} (u_{ij} - \bar{u})(u_b - \bar{u}), \quad (5)$$

with b consisting of all $N_{ij}=4$ elements of a von Neumann neighborhood at each lattice site u_{ij} . Using different local neighborhoods for b does not change the results qualitatively. The spatial cross correlation is given by

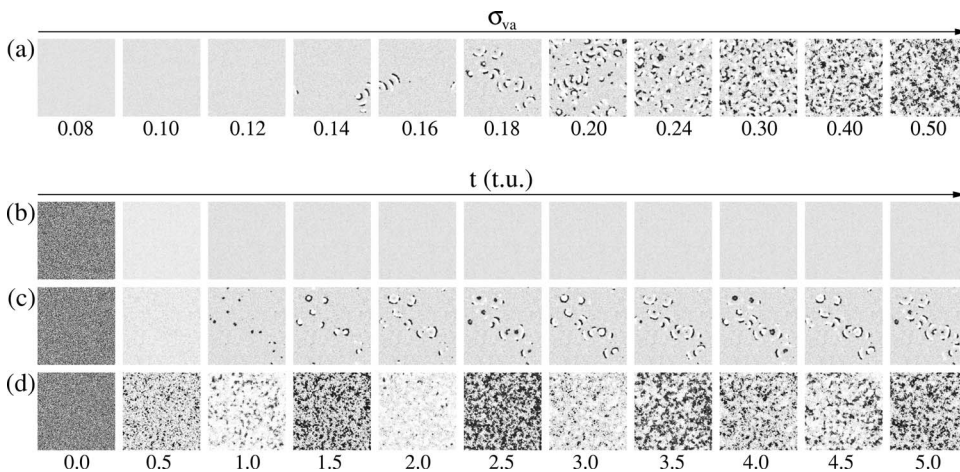


FIG. 4. Snapshots of $u_{ij}(t)$ from Eq. (1) with random initial conditions: (a) dependent on the variability strength σ_{va} after $t = 40$ t.u. (b)–(d) dependent on t ; $\sigma_{va} =$ (b) 0.1, (c) 0.18, and (d) 0.5. Other parameters: $C=2.93$, $\sigma_{vm}=0$.

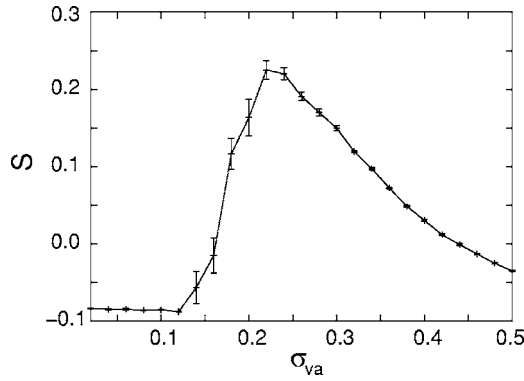


FIG. 5. The cross-correlation measure S [Eq. (6)] for a net of FitzHugh-Nagumo elements [Eq. (1)] averaged over ten realizations of the net, dependent on the variability strength σ_{va} ; total integration time $T=40$ t.u. Other parameters: $C=2.93$, $\sigma_{vm}=0$.

$$S = \left\langle \frac{K(t)}{V(t)} \right\rangle_T, \quad (6)$$

where $\langle \cdot \rangle_T$ denotes the time average over the total integration time T . S is a measure for the relative change of the order of a spatially extended system. If the net is completely synchronized in space and time one gets the maximum value $S=1$. For a completely asynchronous net dynamics one receives $S=0$ and for a strongly anticorrelated dynamics the spatial cross correlation takes up a minimum value of -1 .

Applying the spatial cross-correlation measure S (Fig. 5) one clearly sees that the coherence of the observed pattern formation shows a resonancelike behavior with increasing variability strength σ_{va} . One can clearly discern a resonance curve with a maximum at $\sigma_{va} \approx 0.22$. At first view this phenomenon looks similar to STSR induced by additive white noise, but the development of the patterns is different and so are the observed structures. In the case of noise-induced STSR the stochastic external driver randomly excites elements in the net. The excited elements act as excitation centers from which the waves spread through the medium. The excitation centers are not fixed and thus the patterns change their shape strongly in time. In the case without noise but with additive variability one increases the diversity between the elements inside the net with growing σ_{va} . For $\sigma_{va} < 0.03$, nevertheless, nearly all elements are excitable (Fig. 3). This changes for higher variability strengths, where a reasonable amount of elements becomes oscillatory. These elements are, however, bound to the spatiotemporally uniform solution of the net for $\sigma_{va} \leq 0.12$. For higher variability strengths the diversity in the net is large enough to destroy the spatially uniform temporally constant net dynamics. Single elements or small clusters of elements in the net start to oscillate. These oscillating elements now act as excitation centers from which the waves spread through the otherwise subexcitable net. If the additive variability strength is further increased a weak coupling is not able to conserve an ordered net dynamics anymore and the dynamics of the single elements become more and more dominant. The coherent structures get destroyed [Fig. 4(d)]. For a subexcitable net with

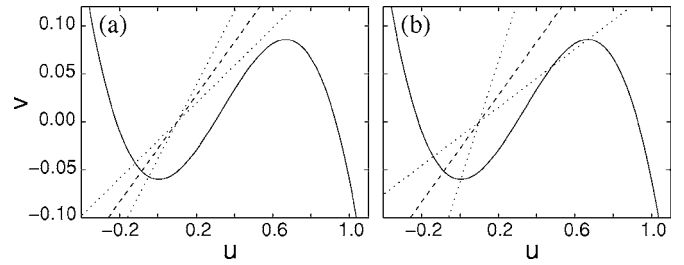


FIG. 6. Nullclines for one FitzHugh-Nagumo element [Eq. (1)]; (—) cubic nullcline, (---) linear nullcline for $c_{ij}=C$. (···) linear nullclines for $c_{ij} =$ (a) $C \pm 1.5$ and (b) $C \pm 3.0$. Other parameters: $C=3.6$, $e_{ij}=-0.1$.

larger coupling strengths ($q > 20$) the observed phenomena are shifted to larger variability strengths.

IV. MULTIPLICATIVE VARIABILITY

In this section we use the parameter values $C=3.6$ and $\sigma_{va}=0$. The variability strength σ_{vm} and the coupling strength q are varied. For the chosen parameters and without multiplicative variability each FHN element again has only one stable fixed point (Fig. 1), resulting in a spatially uniform temporally constant solution of the net and any initial conditions. Again the net is subexcitable, but not as close to the transition to the excitable dynamics as in Sec. III, because of a different value of C .

In contrast to variability in the parameter e multiplicative variability changes the slope of the linear nullcline (Fig. 6); this again has an influence on the dynamics of a single element (Fig. 1). For $1.58 \leq c_{ij} \leq 6.32$ the element is in the excitable regime. For other values of c_{ij} other dynamical regimes are realized. For $c_{ij} < 0$ the slope of the linear nullcline is negative and the dynamics of the element completely changes. Consequently, the parameter values $c_{ij} < 0$ have to be excluded by setting the probability distribution $P(c, \sigma_{vm})$ to zero for corresponding values of c . For the largest variability strength used in this paper this would affect 10% of the random values generated with a normal Gaussian distribution. Similar to the net with variability in the parameter e , the net [Eq. (1)] with variability in the parameter c consists of elements in different dynamical regimes. In a net of Hodgkin-Huxley elements the multiplicative variability would not only cause a shift of the nullclines $n_{ij}(V)$, as for additive variability, but also change their shape (slope).

In [16] it was shown that variability in the parameter c has a systematic effect on the mean gradient angle $\langle \alpha \rangle$ of the linear nullcline of the net. Furthermore, it was demonstrated that this effective mean value can describe a special phase transition (from the oscillatory to the excitable net dynamics) for large nets with strong coupling quite well. An effective mean parameter $\langle c \rangle$ dependent on σ_{vm} can be calculated:

$$\langle c \rangle(\sigma_{vm}) = \frac{1}{\tan[\langle \alpha \rangle(\sigma_{vm})]},$$

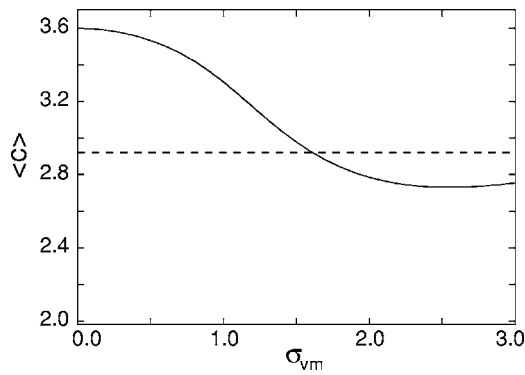


FIG. 7. Effective mean value $\langle c \rangle$ [Eq. (7)] for a net of FHN elements [Eq. (1)], dependent on the variability strength σ_{vm} . (- -) $\langle c \rangle = 2.92$ expected transitions to an excitable net for $q = 20$. Other parameters: $C = 3.6$.

$$\langle \alpha \rangle(\sigma_{vm}) = \int_{-\infty}^{\infty} \alpha(c) P(c, \sigma_{vm}) dc. \quad (7)$$

Thereby $\alpha(c)$ is the gradient angle of the linear nullcline, which depends only on the parameter c .

The global net parameter $\langle c \rangle(\sigma_{vm})$, for the parameter values chosen in this section, is presented in Fig. 7. Starting from $\langle c \rangle(0) = 3.6$ the effective parameter drops with increasing strength of the multiplicative variability, reaching a value of 2.92 for $\sigma_{vm} \approx 1.6$. For a net without variability one finds the transition from the subexcitable to the excitable net dynamics for a parameter value $c = 2.92$ for $q = 20$ (the transition point depends on q ; see also Fig. 9). If $\langle c \rangle$ determines the net dynamics one would thus expect to find a transition to the excitable behavior for $\sigma_{vm} \approx 1.6$ and an appropriate coupling strength. For different values of q the transition point changes, but one would still expect to find the transition. For $\sigma_{vm} \approx 2.5$ the curve $\langle c \rangle(\sigma_{vm})$ has a minimum and is rising for larger variability strengths. This is caused by the cutoff of $P(c, \sigma_{vm})$ for $c < 0$.

To study the effects of the variability in parameter c numerical simulations varying the variability strength σ_{vm} and the coupling strength q are performed. Starting with random initial conditions no pattern formation is observed in the net for the examined parameter range ($5 < q < 100$ and $0 < \sigma_{vm} < 4$). In contrast to additive variability excitation waves are not induced by variability in parameter c . The spatially uniform temporally constant solution of the net stays stable.

In the next step the simulations are repeated with special initial conditions, which induce two spiral waves in the net. In a subexcitable medium these waves die out quickly, whereas in an excitable net the induced waves are sustained and can be observed even for long integration times. The results after a propagation time of 40 t.u. are displayed in Fig. 8. For $q \leq 20$ the induced waves are not preserved in the net for any variability strength σ_{vm} and the net stays subexcitable. The excitable pattern-forming regime is found only for $q > 20$ and an appropriate variability strength σ_{vm} .

The border of the excitable regime is identified using simulations of ten different net realizations over a total inte-

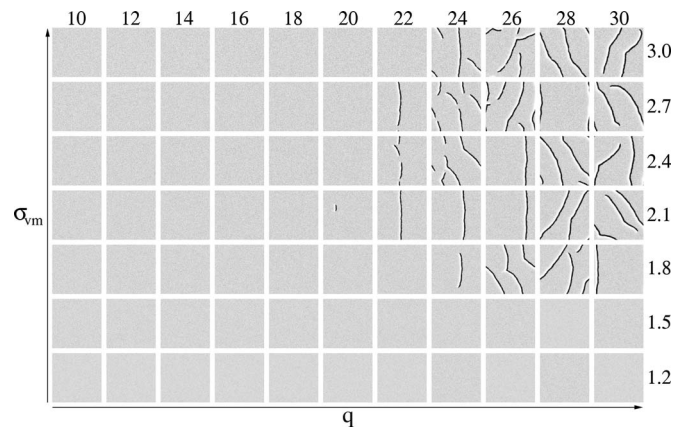


FIG. 8. Snapshots of $u_{ij}(t)$ from Eq. (1) after $t = 40$ t.u.; special initial conditions induce two spiral waves in an excitable net, dependent on the variability strength σ_{vm} and the coupling strength q . Other parameters: $C = 3.6$, $\sigma_{va} = 0$.

gration time of $T = 100$ t.u. The results, dependent on the relevant parameters σ_{vm} and q , are presented in Fig. 9. As mentioned above the transition does not occur for coupling strengths $q \leq 20$. For larger coupling strengths the net becomes excitable for sufficiently large variability strengths. For a strong coupling $q \geq 25$ the q -dependent transition to excitable net dynamics can be predicted well using Eq. (7). Thus the effective parameter $\langle c \rangle$ describes the net dynamics for strong coupling. Once in the excitable regime a further increase of σ_{vm} has a disordering influence, leading to a destruction of the patterns and the excitable net dynamics (dependent on q).

The strong dependence on the coupling strength q of the observed transition can be explained. The transition is generated by the systematic effect of the multiplicative variability [Eq. (7)]. This is, however, not the only effect of the variability. It also has a disordering effect, which is dominant for a weak coupling, whereas for larger coupling strengths this disordering effect gets more and more suppressed. In the case of a strong coupling the elements are strongly bound to each other and the effective mean value $\langle c \rangle$ determines the global net dynamics, for not too large variability strengths. Thus the transition to excitable dynamics can only be ob-

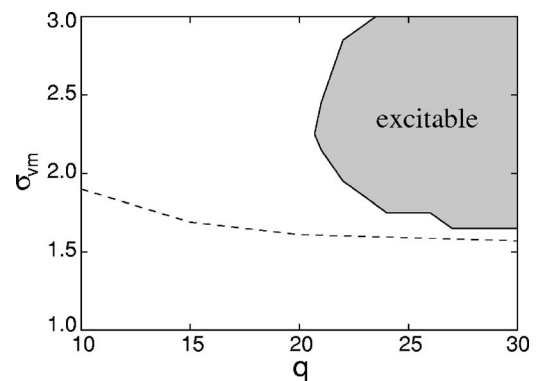


FIG. 9. Border of the excitable regime for Eq. (1), dependent on the variability strength σ_{vm} and the coupling strength q . (- -) Transition predicted by Eq. (7). Other parameters: $C = 3.6$, $\sigma_{va} = 0$.

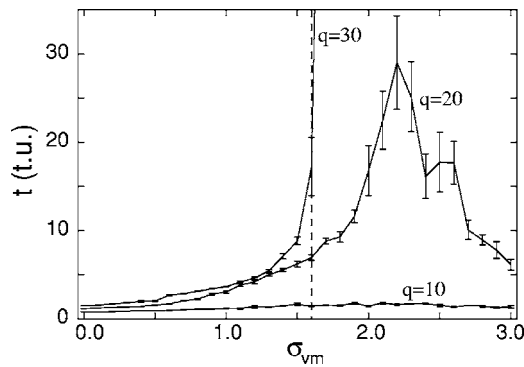


FIG. 10. Lifetime of two spiral waves induced by special initial conditions in a net of FitzHugh-Nagumo elements [Eq. (1)], averaged over ten realizations of the net, dependent on the variability strength σ_{vm} for three different coupling strength q . (—) Transition predicted by Eq. (7) for coupling strength $q=30$. Other parameters: $C=3.6$, $\sigma_{va}=0$.

served for a sufficiently large coupling. For smaller coupling strengths the net stays subexcitable, but the multiplicative variability may nevertheless have systematic effects on the observed net dynamics.

One net property that is systematically influenced by the variability in parameter c is the lifetime of the initialized waves (Fig. 8). This lifetime is presented in Fig. 10 for three different values of the coupling strength q . For $q=10$ no effect on the lifetime of the waves is observed. This is also true for additive variability, which has no systematic effect on the net (not presented in the figure). For the strong coupling strength $q=30$ one observes a monotonic growth of the lifetime with increasing variability strength σ_{vm} . At the border to the excitable net dynamics the lifetime tends to infinity. More interesting is the intermediate coupling strength $q=20$. For this value one observes a strong increase in the lifetime with growing variability strength starting from σ_{vm}

$=0$, but the lifetime does not diverge (no transition). After a sharp maximum the lifetime is lessened with a further increase of σ_{vm} . This means that for an intermediate coupling strength and an intermediate variability strength σ_{vm} the lifetime of waves in a subexcitable medium is strongly enhanced.

V. SUMMARY

In this paper it was shown that additive variability is able to induce pattern formation in a subexcitable net of FHN elements. This variability-induced structure formation exhibits a resonancelike dependence on the variability strength σ_{va} . The response of the net to multiplicative variability is very different. In this case no pattern formation is induced, but one observes a systematic influence on the net dynamics. This effect causes a transition to excitable dynamics for a coupling strength $q > 20$ and it enhances the lifetime of patterns in the subexcitable net for an intermediate coupling strength. For a strong coupling the effective net parameter $\langle c \rangle(\sigma_{vm})$ determines the net dynamics and predicts the transition quite accurately.

These results demonstrate that variability may play an important role in biophysical systems. Variability could be essential for pattern formation mechanisms or stochastic resonance effects. At least it may influence noise-induced effects, such as temporal or spatiotemporal stochastic resonance. Multiplicative variability has in addition a systematic effect, which could cause a wide range of interesting phenomena, like variability-induced phase transitions. The effects of variability have been studied using the paradigmatic FHN model in a rather general framework. We hope that these theoretical findings will contribute to the theory of extended systems influenced by variability (diversity) and noise [8]. Beyond this we hope that this work may foster experimental research in this field.

-
- [1] P. Jung and G. Mayer-Kress, *Phys. Rev. Lett.* **74**, 2130 (1995).
 - [2] P. Jung, A. Cornell-Bell, F. Moss, S. Kádár, J. Wang, and K. Showalter, *Chaos* **8**, 567 (1998).
 - [3] H. Busch and F. Kaiser, *Phys. Rev. E* **67**, 041105 (2003).
 - [4] A. S. Pikovsky and J. Kurths, *Phys. Rev. Lett.* **78**, 775 (1997).
 - [5] S. Kádár, J. Wang, and K. Showalter, *Nature (London)* **391**, 770 (1998).
 - [6] S. Alonso, I. Sendina-Nadal, V. Perez-Munuzuri, J. M. Sancho, and F. Sagues, *Phys. Rev. Lett.* **87**, 078302 (2001).
 - [7] E. A. Novikov, *Sov. Phys. JETP* **20**, 1920 (1964).
 - [8] J. García-Ojalvo and J. M. Sancho, *Noise in Spatially Extended Systems* (Springer, Berlin, 1999).
 - [9] E. Ullner, A. Zaikin, J. García-Ojalvo, and J. Kurths, *Phys. Rev. Lett.* **91**, 180601 (2003).
 - [10] E. Glatt, H. Busch, F. Kaiser, and A. Zaikin, *Phys. Rev. E* **73**, 026216 (2006).
 - [11] A. T. Winfree, *J. Theor. Biol.* **16**, 15 (1967).
 - [12] Y. Kuramoto, *Chemical Oscillations, Waves and Turbulence* (Springer, Berlin, 1984).
 - [13] A. Pikovsky, M. Rosenblum, and J. Kurths, *Synchronization. A Universal Concept in Nonlinear Sciences* (Cambridge University Press, Cambridge, U.K., 2001).
 - [14] Y. Braiman, J. F. Lindner, and W. L. Ditto, *Nature (London)* **378**, 465 (1995).
 - [15] M.-T. Hütt, H. Busch, and F. Kaiser, *Nova Acta Leopold.* **332**, 381 (2003).
 - [16] E. Glatt, M. Gassel, and F. Kaiser, *Phys. Rev. E* **73**, 066230 (2006).
 - [17] C. J. Tessone, C. R. Mirasso, R. Toral, and J. D. Gunton, *Phys. Rev. Lett.* **97**, 194101 (2006).
 - [18] J. S. Nagumo and S. Yoshizawa, *Proc. IRE* **50**, 2061 (1962).
 - [19] J. Moehlis, *J. Math. Biol.* **52**, 141 (2006).
 - [20] A. L. Hodgkin and A. F. Huxley, *J. Physiol. (London)* **117**, 500 (1952).